Bioorganic & Medicinal Chemistry 19 (2011) 7698–7710

Contents lists available at SciVerse ScienceDirect

Bioorganic & Medicinal Chemistry

journal homepage: www.elsevier.com/locate/bmc

Synthesis and in vitro evaluation of fluorinated styryl benzazoles as amyloid-probes

Goreti Ribeiro Morais [a,†], Hugo Vicente Miranda [b,†], Isabel C. Santos [a], Isabel Santos [a], Tiago F. Outeiro [b,c,d,*], Antonio Paulo [a,*]

[a] Unidade de Ciências Químicas Radiofarmacêuticas, Instituto Tecnológico e Nuclear, Estrada Nacional 10, 2686 953 Sacavém, Portugal
[b] Cell and Molecular Neuroscience Unit, Instituto de Medicina Molecular, Av. Prof. Egas Moniz, 1649 028 Lisboa, Portugal
[c] Instituto de Fisiologia, Faculdade de Medicina da Universidade de Lisboa, Lisboa, Portugal
[d] Department of Neurodegeneration and Restaurative Research, University Medizin Göttingen, Waldweg 33, 37073 Göttingen, Germany

ARTICLE INFO

Article history:
Received 7 July 2011
Revised 23 September 2011
Accepted 28 September 2011
Available online 18 October 2011

Keywords:
Benzazoles
Styryl derivatives
Wittig reaction
Fluorescence
Amyloid fibrils
Binding affinity

ABSTRACT

The formation of proteinaceous aggregates is a pathognomonic hallmark of several neurodegenerative disorders such as Alzheimer's and Parkinson's diseases. To date, the final diagnostic for these diseases can only be achieved by immunostaining of post-mortem brain tissues with the commonly used congo red and Thioflavin T/S amyloid-dyes. The interest in developing amyloid-avid radioprobes to be used for protein aggregates imaging by positron emission tomography has grown substantialy, due to the promise in assisting diagnosis of these disorders. To this purpose, the present work describes the synthesis and characterization of four novel fluorinated styryl benzazole derivatives **1**–**4** by means of the Wittig reaction, as well as their in vitro evaluation as amyloid-probing agents. All compounds were obtained as mixtures of geometric *E* and *Z* isomers, with the preferable formation of the *E* isomer. Photoisomerization reactions allowed for the maximization of the minor *Z* isomers. The authentic **1**–**4***E*/*Z* isomers were isolated after purification by column chromatography under dark conditions. Profiting from the fluorescence properties of the different geometric isomers of **1**–**4**, their binding affinities towards amyloid fibrils of insulin, α-synuclein and β-amyloid peptide were also measured. These compounds share similarities with Thioflavin T, interacting specifically with fibrillary species with a red-shift in the excitation wavelengths along with an increase in the fluorescence emission intensity. Apparent binding constants were determined and ranged between 1.22 and 23.96 μM^{-1}. The present data suggest that the novel fluorinated styryl benzazole derivatives may prove useful for the design of ^{18}F-labeled amyloid radioprobes.

1. Introduction

Neurodegenerative diseases, such as Alzheimer's (AD) or Parkinson's diseases (PD), are highly debilitating conditions affecting millions of people worldwide. These disorders are commonly known as 'protein misfolding disorders' as they are characterized by the accumulation of insoluble protein aggregates. Although the molecular processes underlying these pathologies are still unknown, β-amyloid (Aβ) plaques and tau neurofibrillary tangles in AD, and Lewy bodies mainly composed of alpha-synuclein (α-syn) in PD, are thought to play a central role in these disorders.

To date, definitive confirmation of AD or PD is only possible upon post-mortem histopathologic studies, using antibodies and dyes such as Thioflavin T (ThT) (Fig. 1) or Congo red that stain such deposits.[1] Thus, the in vivo visualization by noninvasive molecular imaging techniques of the deposits, which are thought to accumulate prior to the overt manifestation of the typical clinical symptoms of these diseases, would enable early diagnosis and the evaluation of the effects of anti-amyloidogenic based therapies. Positron emission tomography (PET) is among the best suited molecular imaging modalities to achieve such a goal, if available amyloid-avid radioprobes can cross the blood brain barrier. Several planar and nonionic molecules (Fig. 1) were designed, labeled with the PET radioisotopes ^{11}C ($t_{1/2}$ = 20 min) and ^{18}F ($t_{1/2}$ = 110 min), and clinically evaluated in humans, in order to generate radioprobes for the in vivo targeting of Aβ plaques in the brain. Their molecular target is not the Aβ peptide sequence per se, but the generic β-sheet structure forming amyloid folds, which can also be formed by a range of other proteins (e.g., α-syn, and insulin).[2] Hence, the amyloid binding profile of the compounds is a crucial issue in the development of PET radiotracers for in vivo imaging of amyloid aggregates.

The benzothiazole derivative [^{11}C]PIB (Fig. 1), designated commonly as Pittsburgh compound B (PIB), is the best characterized PET radiotracer for in vivo β-amyloid imaging.[3] However, the short half-life of ^{11}C limits its use to centers with an on-site cyclotron.

* Corresponding authors. Tel.: +351 21 9946196; fax: +351 21 994 6185 (A.P.).
E-mail addresses: touteiro@gmail.com (T.F. Outeiro), apaulo@itn.pt (A. Paulo).
† These authors contributed equally to this work.

0968-0896/$ - see front matter © 2011 Elsevier Ltd. All rights reserved.
doi:10.1016/j.bmc.2011.09.065

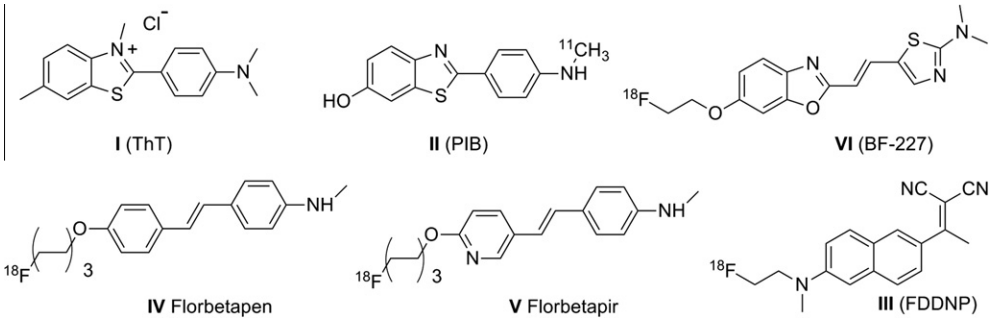

Figure 1. Chemical structures of relevant Aβ binding agents.

Such limitation prompted several authors to search for alternative compounds radiolabeled with the long-lived ^{18}F, namely radiofluorinated stilbenes and styrylpyridines (see compounds **IV** and **V** in Fig. 1).[4] Like benzothiazoles, these styryl derivatives are planar molecules with extended π-delocalized systems, which enable their insertion between the β sheets of amyloid aggregates. Some of these styryl derivatives were able to target in vivo Aβ plaques but exhibited to some extent nonspecific retention in the brain. Therefore, it is important to identify better performing PET probes for selective in vivo imaging of amyloid deposits.

We focused on fluorinated styryl benzazole derivatives as small, planar and π-delocalized compounds to design ^{18}F-labeled probes for PET imaging of amyloid aggregates. Herein, we report the synthesis and characterization of four novel fluorinated styryl-containing compounds (**1**–**4**) of the benzothiazole, benzoxazole and benzimidazole type (Fig. 2), which were isolated as the respective *E* and *Z* isomers. We also report on the fluorescence properties of the different geometric isomers of **1**–**4**, as well as on their binding affinities towards amyloid aggregates of insulin, α-syn and Aβ(1–42) peptide, which were measured by in vitro binding assays using fluorescence spectroscopy. We assessed the influence of the different heteroatoms (N vs O vs S) on the affinity of styryl-benzazole derivatives towards different types of amyloid structures, aiming to have a first insight into the relevance of these compounds for the design of ^{18}F-labeled probes for in vivo targeting of amyloid aggregates.

2. Results and discussion

2.1. Synthesis

Several approaches can be undertaken to prepare styryl benzazole derivatives, namely those based on the Knoevenagel, Horner–Wadsworth–Emmons and Wittig reaction.[5–20] In this work, the olefin bond of the styryl benzazole derivatives **1**–**4** was fashioned via the Wittig reaction of benzazolylmethylenetriphenylphosphoranes with substituted benzaldehydes. This involved the synthesis of benzazolylmethyltriphenylphosphonium salts, **11**–**13**, as key intermediates (Scheme 1) to generate the corresponding phosphoranes. Compounds **11** and **13** have been previously used for the synthesis of styryl derivatives.[6,21,22] The synthesis of **11**–**13** started with the preparation of the respective 2-chloromethylbenzazoles **8**–**10** by condensation of the commercially available o-substituted phenyl amines **5**–**7** with chloroacetic acid, using suitable catalysts.[6,23,24]

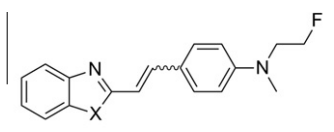

Figure 2. Structure of the new fluorinated styryl benzazole derivatives.

Reaction of **8** and **9** with triphenylphosphine in refluxing toluene afforded, in excellent yields, benzothiazolylmethyltriphenylphosphonium chloride **11** and benzoxazolylmethyltriphenylphosphonium chloride **12**, respectively. The more polar benzimidazolylmethyltriphenylphosphonium chloride **13** was obtained in a similar way but the reaction was carried out in acetonitrile. The benzoxazolylmethyltriphenylphosphonium chloride **12** is a new compound that has been fully characterized by NMR techniques (^1H, ^{13}C and ^{31}P), and by X-ray diffraction analysis (Fig. 3).

For the benzothiazole- and benzoxazole-containing compounds, the Wittig reaction leading to the styryl benzazoles (see below) could be performed using the *O*-tosylate derivative **15**[25] obtained from the commercially available **14** (Scheme 2). By contrast, for the benzimidazoles, the Wittig reaction was performed using the *O*-*tert*-butylcarbonate derivative **16**, prepared as described in Scheme 2. After the condensation reaction, removal of the base-resistant O-protective group was followed by the preparation of tosylated derivatives, as described below. These strategies allowed for a convergent synthesis of the desired fluorinated styryl benzazole derivatives **1**–**4** via nucleophilic substitution (Schemes 2–4).

Treatment of **11** and **12** with potassium *tert*-butoxide in benzene gave the respective phosphoranes **17** and **18**. Like the previously reported **17**,[21] the new phosphorane **18** is not very stable and was prepared just prior to use. The Wittig reactions of **17** and **18** with **15** afforded the styrylbenzothiazole **19** and styrylbenzoxazole **20** in 89% and 65% yields, respectively (Scheme 3). Compounds **19** and **20** were isolated as a mixture of *E* (**19**-*E* and **20**-*E*) and *Z* (**19**-*Z* and **20**-*Z*) isomers in a ratio of around 95:5. *Z* and *E* geometry was confirmed by the proton–proton coupling constants ($J_{H,H}$) of 12.3 and 16.5 Hz that were found for the respective olefinic protons. Reaction of **19**-*E*/**19**-*Z* and **20**-*E*/**20**-*Z* with tetrabutylammonium fluoride (TBAF) in refluxing THF gave the respective mixtures of **1**-*E*/**1**-*Z* and of **2**-*E*/**2**-*Z* in good yield.

The synthesis of the structurally related styryl benzimidazole **3** involved the reaction of the corresponding phosphorane, prepared in situ by treating **13** with sodium methoxide in dry methanol with the Boc-protected benzaldehyde **16** (Scheme 4). This reaction afforded the styryl benzimidazole derivative **21** in good yield, which was obtained as a mixture of the geometric isomers **21**-*E* and **21**-*Z* in a *E*/*Z* ratio of 70:30. Hydrolysis of the Boc-protecting group of compounds **21**-*E*/**21**-*Z* (mixture) under acid catalysis, followed by neutralization of the reaction mixture with triethylamine and by a 30 min reaction with *p*-toluenesulfonyl chloride, afforded authentic **22**-*E* in a yield of 32%. The low yield of **22** was due to the short reaction time used to prevent the *N*-tosylation of the benzimidazole ring. Under these conditions only the less steric hindered *E* isomer was transformed into the tosylate derivative. The reaction of **22**-*E* with TBAF in refluxing THF gave the final fluorinated styryl benzimidazole **3**, which was obtained as a mixture of *E*/*Z* isomers with a poor yield of 16%. This low yield could be explained by competitive nucleophilic alkylation reactions involving the deprotonated amine of the benzimidazole ring, which led to the formation of unidentified by-products.

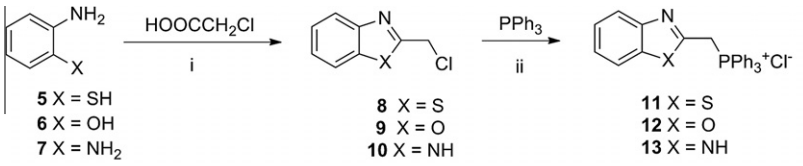

i. CH_3SO_2H/SiO_2 for **8**, PPA for **9** and 4N HCl for **10**; ii. toluene for **11** and **12** and acetonitrile for **13**

Scheme 1. Synthesis of the phosphonium derivatives.

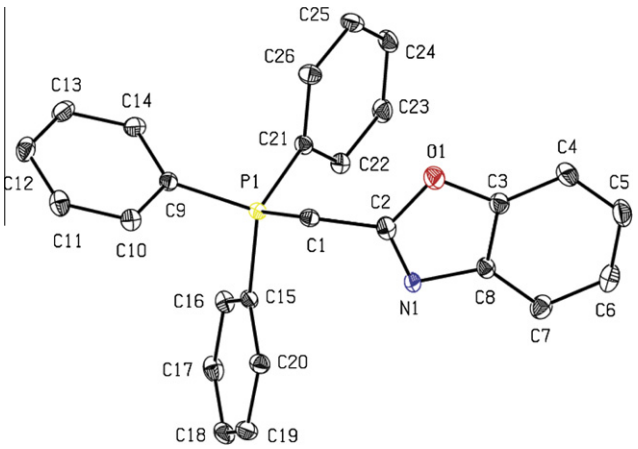

Figure 3. ORTEP view of the cation of 2-benzoxazolylmethyltriphenylphosphonium chloride **12**.

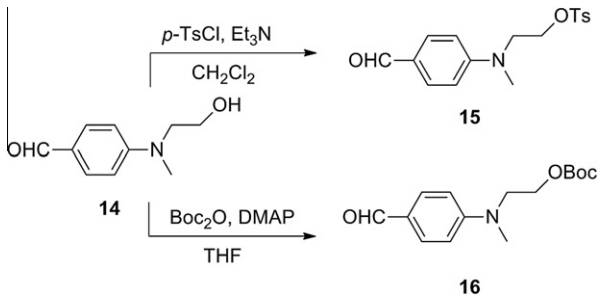

Scheme 2. Synthesis of *O*-substituted benzaldehyde derivatives.

Treatment of the mixture **21**-*E*/**21**-*Z* with 1.5 equiv of methyl iodide under phase transfer conditions[9] gave the respective *N*-methylated analogs **23**-*E*/**23**-*Z* in quantitative yield (Scheme 4). The *O*-tosylation of **23**-*E*/**23**-*Z* afforded **24**-*E*/**24**-*Z* compounds in a similar manner as described for **22**-*E*. Due to the absence of competitive N-alkylation reactions, compounds **24**-*E*/**24**-*Z* were obtained with a yield of 69%. Finally, the desired fluorinated styryl *N*-methyl benzimidazole **4** was obtained in excellent yield (80%) when **24** was reacted with TBAF in refluxing THF.

To improve the final yield of **3** we have explored other strategies. First, we have studied the synthesis of the *O*-tosylated intermediate **22** by the base-free direct condensation of 2-methylbenzimidazole with **15** at 200 °C in a sealed tube, to overcome the competitive *N*-tosylation.[8] However, this reaction did not proceed with the formation of **22** as shown by the ^{1}H NMR analysis of the reaction crude. Another alternative consisted on the reaction of *o*-phenylidenediamine **7** with the fluorinated cinnamic acid derivative **25**, which was obtained from **15** in three steps (Scheme 5).[26] This condensation reaction, catalyzed by PPA, also formed **3** in low yield (10–20%) and, therefore, was not a better alternative for the synthesis of this compound. This bad outcome was not improved by using a larger molar excess of **25**, longer reaction times or higher temperatures (200 °C).

2.2. Photochemical interconversion of *E*/*Z* isomers

As described, the final fluorinated styryl-benzazoles **1**–**4** were obtained as a mixture of geometric *E*/*Z* isomers, being dominant the *E* isomer. The *E*/*Z* ratio of the different styryl-benzazoles described in this work changed when the compounds were kept in solution and exposed to day light, in agreement with the ability of styryl benzazoles to undergo photoisomerization.[15,27] For instance, ^{1}H NMR analysis of a solution of **4** in chloroform showed that the initial **4**-*E*/**4**-*Z* ratio of 2.6:1 changed to a 1:19 ratio, after 2 days of light exposure. After this time the *E*/*Z* ratio reached equilibrium. A similar behavior was observed for the other fluorinated styryl-benzazoles **1**–**3** in chloroform solution. For all compounds, there is a preference towards the formation of the *Z* isomer by photoisomerization. Thus, the formation of the minor *Z* isomer of **1**–**4** was maximized by exposing the mixtures *E*-**1**–**4**/*Z*-**1**–**4** to light for 48 h. With the exception of **3**-*Z*, each isomer was purified by column chromatography under dark conditions, as described in the experimental section.

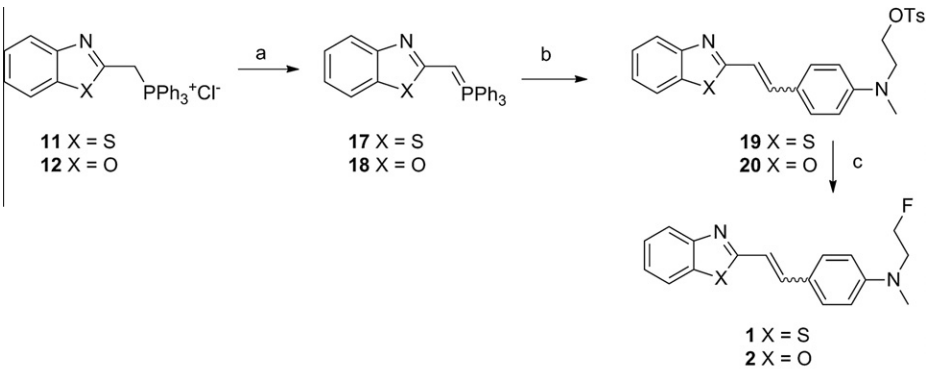

a) K^{t}BuO, benzene; b) **15**, THF; c) TBAF, THF

Scheme 3. Synthesis of fluorinated styryl benzazoles **1** and **2**.

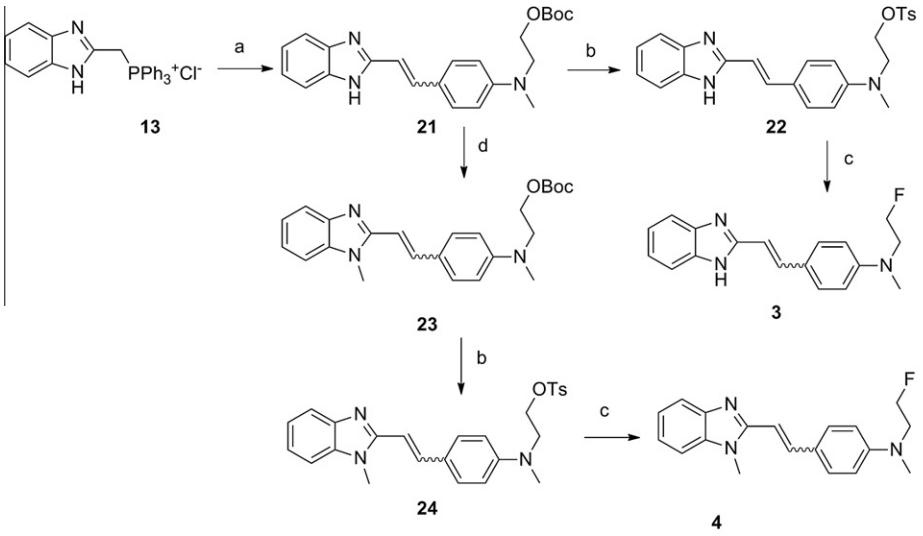

a) NaOMe, MeOH, **16**; b) i, TFA, CH_2Cl_2, ii. *p*-TsCl, Et_3N, CH_2Cl_2; c) TBAF, THF; d) MeI, acetone, aq. NaOH

Scheme 4. Synthesis of fluorinated styryl benzimidazoles **3** and **4**.

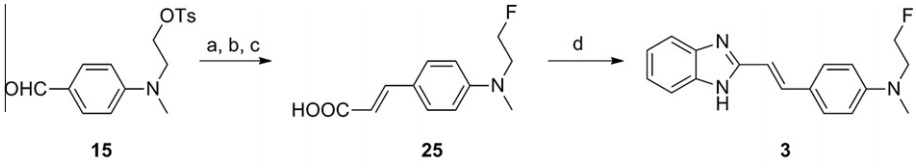

a) $EtOOCHPPh_3$, $CHCl_3$; b) 1N HCl; c) TBAF, THF; d) PPA

Scheme 5. Alternative synthesis of the fluorinated styryl benzimidazole **3**.

2.3. Intrinsic fluorescence characteristics and interaction with amyloid fibrils

Profiting from the intrinsic fluorescence properties of the fluorinated styryl-benzazole derivatives **1**–**4**, we tested their binding ability towards amyloid fibrils formed by insulin, α-syn and Aβ(1–42), all of which are known to form typical amyloid aggregates with common 'cross-β' architecture. Fibrillization was induced by standard procedures and the interaction of authentic *E* and *Z* isomers of **1**–**4** with the resulting aggregated species was studied in order to assess the influence of isomerism on the binding abilities of the compounds. This influence has been previously assessed for styrylbenzene derivatives,[28] but, so far, no similar studies were reported for styryl-benzazole derivatives. The isomer **3**-*Z* was not evaluated in this study, as its counterpart **3**-*E* was obtained in a quite poor yield and its photoisomerization did not provide the required amount of **3**-*Z*.

The authentic *E* and *Z* isomers share similar fluorescence properties, displaying similar maximum excitation and emission wavelengths for the interaction with monomers and fibrils (Table 1). Upon interaction with fibrils, we observed an increase in fluorescence intensity that was proportional to the concentration of amyloid fibrils (Fig. 4, Table 2), in agreement to what is observed upon ThT binding to amyloid fibrils.[29,30] For all the compounds, the interaction with the different fibrillary species led to a red-shift in the excitation wavelength. By contrast, the emission properties varied slightly depending on the type of amyloid fibrils. The interaction of the *E* and *Z* isomers of **1** and **2** and isomer **3**-*E* with insulin fibrils caused a red-shift in their emission maximum, while for the same compounds the interaction with α-syn fibrils led to a blue shift. On the other hand, we observed a blue-shift upon binding to insulin fibrils of compounds **4**-*Z* and **4**-*E*, which did not suffer any change on their emission wavelength following the interaction with α-syn. Unlike **3**-*E*, all the other fluorinated styryl-benzazoles undergo a blue-shift in emission upon binding to Aβ(1–42) fibrils.

To directly measure the fibril-binding properties of the compounds, fluorescence intensity binding assays were performed by using a fixed concentration of fibrils (3.5 to 11.35 μM) and varying concentrations of ligands (2.25 to 13.5 μM) (Fig. 5). The binding constants were obtained by single site saturated curve fitting to the fluorescence data as a function of the ligand concentration. The calculated Kd values are in the μM range spanning between 1.22 and 23.96 μM^{-1} (Table 3) while for ThT the range is between 2.43 and 11.93 μM^{-1}. These apparent Kd values are in the same order of magnitude as those previously reported for ThT, the most widely used dye for cross β-sheet structure detection.[31,32] Moreover, the Kd values of compounds **1**–**4** are in the same order of magnitude as the values reported for other compounds with potential as amyloid-avid PET radioprobes, when obtained directly by intrinsic fluorescence intensity binding assays.[33,34] There is an influence of the nature of the heteroatom and type of geometric isomer on the binding abilities of the compounds but a clear trend could not be identified due to a few exceptions. In general, the benzothiazole derivatives tend to exhibit the lowest affinity towards the different types of amyloid fibrils. However, among all the tested compounds the styryl-benzothiazole ***1***-*E* has shown the highest affinity for α-syn aggregates. For the different amyloid fibrils the *E* isomers show a higher affinity than the *Z* counterparts, being the affinity of **4**-*Z* and **4**-*E* towards aggregates of Aβ(1–42) the unique exception to this trend. However, the Kd values found

Table 1
Fluorescence maximum excitation and emission wavelengths of the *E* and *Z* geometric isomers of compounds **1**–**4** in the presence of monomeric and fibrillary insulin, α-syn, and Aβ(1–42) and unbound dye (free)

	Insulin				α-syn				Aβ(1–42)				Free	
	Monomer		Fibrils		Monomer		Fibrils		Monomer		Fibrils			
	$\lambda_{excitation}$ (nm)	$\lambda_{emission}$ (nm)	$\lambda_{excitation}$ (nm)	$\lambda_{emission}$ (nm)	$\lambda_{excitation}$ (nm)	$\lambda_{emission}$ (nm)	$\lambda_{excitation}$ (nm)	$\lambda_{emission}$ (nm)	$\lambda_{excitation}$ (nm)	$\lambda_{emission}$ (nm)	$\lambda_{excitation}$ (nm)	$\lambda_{emission}$ (nm)	$\lambda_{excitation}$ (nm)	$\lambda_{emission}$ (nm)
1-	*Z* 416		538	430	576	416	538	430	518	400	542	418	506	400
	538	**1**-*E*	416	538	430	572	416	544	430	518	400	542	418	510
	400	542												
2-	*Z* 384		508	416	522	384	508	400	498	394	510	400	492	384
	508	**2**-*E*	384	508	416	526	384	508	400	500	394	510	400	492
	384	508												
3-	*E* 372		490	435	516	372	484	384	482	372	484	386	488	394
	516	**4**-*Z*	430	534	454	522	384	488	392	488	380	496	384	490

for each isomer are of the same order of magnitude and, most probably, the occurrence of geometric isomerism should not affect the amyloid-targeting ability of the reported compounds.

Although the interaction of the different compounds with monomers does not result in an increase in the fluorescence intensity signal, we also performed similar titration experiments with a nonamiloydogenic protein (BSA). We have found that no hyperbolic or linear fitting to the experimental data is possible (Fig. S1), given that increasing amounts of dyes concentration do not lead to an increase in the fluorescence intensity. This suggests that **1**–**4** undergo a specific interaction with amyloid fibrils.

In summary, the styryl benzazole derivatives **1**–**4** offer the possibility to bridge the gap between in vitro and in vivo studies involving the targeting of amyloid aggregates. This is due to their intrinsic fluorescence properties and results also from the possibility to obtain the radiofluorinated counterparts, readily available from the tosylated precursors reported herein. Importantly, the lipophilic character of compounds **1**–**4**, displaying log*P* values ranging from 3.95 and 4.83, warrants that the compounds should cross the blood brain barrier, a crucial issue on their ability to reach intracerebral deposits of amyloid. By themselves, they do not emerge as alternative amyloid-fluorescence sensors for the in vitro characterization of amyloid aggregates, as their fluorescence properties are less favorable than those presented by reported fluorescent probes.[35] Nevertheless, the compounds reported herein offer the advantage of a modular synthesis that enables for a versatile introduction of substituents, namely electron-donating groups that can be appended at different positions of the benzazole ring to improve the fluorescence and amyloid-binding properties of the compounds.[36]

3. Conclusion

A series of novel fluorinated styryl benzazole derivatives have been synthesized as potential amyloid-binding agents. Formation of the styryl group has been successfully fashioned by the Wittig reaction, which represents an unprecedented approach in the case of styrylbenzoxazole derivatives. The final fluorinated styryl-benzazole derivatives **1**–**4** were obtained as a mixture of geometric isomers, being the *E* isomer formed preferably. Compounds **1**–**4** are prone to photoisomerize in solution but the extension of isomerization depends on the nature of the azole ring. *E*-benzimidazole styryl derivatives fully isomerize into the *Z* isomer while the counterpart benzothiazole and benzoxazole derivatives undergo only partial isomerization. Taking advantage of the *Z*/*E* photoisomerization ability of these compounds, the different *E* and *Z* isomers of compounds **1**–**4** could be isolated and their binding capabilities towards different types of amyloid fibrils were evaluated in vitro.

Like the benzothiazole dye ThT, the newly synthesized fluorinated derivatives interacted with different amyloid fibrils. These compounds share similarities with thioflavin T, interacting specifically with fibrillary species with a red-shift in the excitation wavelenghts along with an increase in the fluorescence emission intensity. Despite some influence of the azole heteroatom and isomerism, the binding of all compounds to different amyloid fibrils is characterized by Kd values in the μM range. These findings indicate that these compounds display rather similar binding properties to the different insulin, α-syn and Aβ(1–42) fibrillary species, in agreement with the ThT broad cross β-sheet structure recognition.

In conclusion, the present study suggests that the newly synthesized styryl benzazole derivatives hold promise as amyloid fibril detection agents that, once labeled with the positron-emitter ^{18}F, may be explored to design amyloid-avid radioprobes for in vivo detection of amyloid structures typical of neurodegenerative diseases such as AD or PD.

4. Materials and methods

All chemicals and solvents were of reagent grade and were used without purifications unless stated otherwise. NMR spectra were recorded on a Varian Unity 300 NMR spectrometer at the frequencies of 300 MHz (^1H), 75 MHz (^{13}C), 121 MHz (^{31}P) and 282 MHz (^{19}F). Chemical shifts are reported in parts per million. ^1H and ^{13}C chemical shifts were referenced with the residual solvent resonances relative to tetramethylsilane. ^{31}P chemicals shifts were referenced with external 85% H_3PO_4 solution. ^{19}F chemical shifts were referenced externally to α,α′,α″-trifluorotoluene (0.05% in C_6D_6; $\delta = -63.3$). Thin-layer chromatography (TLC) was performed on plates of precoated silica plates 60 F_{254} (Merck). Visualization of the plates was carried out using UV light (254 and 365 nm) and/or iodine chamber. Gravity column chromatography was carried out on silica gel (Merck, 70–230 mesh).

All geometric isomers of the styryl benzazole derivatives were purified by column chromatography under dark. Only authentic *E* and *Z* isomers of **1**–**4** were used to evaluate their fluorescence properties and their binding to the different amyloid fibrils.

The lipophilicity of the final compounds **1**–**4** was estimated by calculating the respective octanol/water partition coefficient (log*P*o/w). The log of the octanol/water partition coefficient (log*P*o/w) of compounds **1**–**4** was calculated using Molecular Operating Environment (MOE) software (Chemical Computing Group, Canada) from the structures optimized with a modified MMFF94.[37] The log*P*(o/w) was calculated by MOE from a linear atom type model (with $r^2 = 0.931$, RMSE = 0.393 on 1,827 molecules).

4.1. 2-Benzoxazolylmethyltriphenylphosphonium chloride (12)

A solution of **9** (173 mg, 1.0 mmol) and triphenylphosphine (263 mg, 1.0 mmol) in toluene (1.6 mL) was refluxed overnight. Thereafter, the formed precipitate was filtered off and was washed several times with ethyl acetate to give **12** (340 mg, 79%)—^1H NMR (CD_3OD, 300 MHz): $\delta = 5.76$ (d, $J = 15.4$ Hz, 2H), 7.48–8.10 (m,

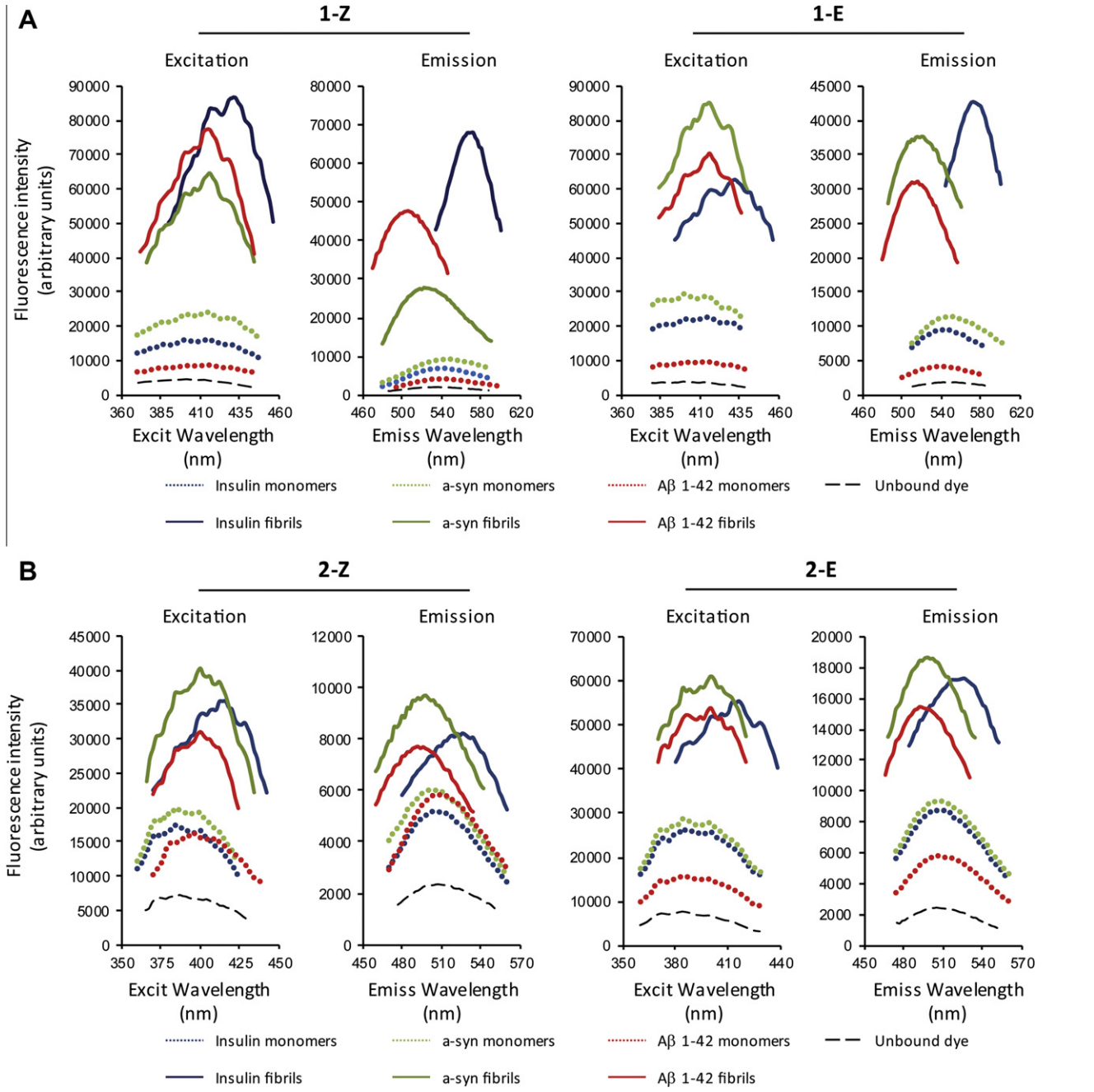

Figure 4. Fluorescence spectra of the *E* and *Z* geometric isomers of the fluorinated styrylbenzazole derivatives **1**–**4** (9 μM) in the absence/presence of monomeric and fibrillary α-syn, insulin and Aβ(1–42) species (2.25 μM). The excitation and emission spectra were taken with fixed maximum excitation and emission wavelengths for the different species according to Table 1.

19H); ^{13}C NMR (CD_3OD, 75 MHz): δ = 111.65, 118.46, 119.63, 121.05, 126.30, 127.34, 131.39, 131.56, 135.14, 135.28, 136.73, 136.77, 141.88; ^{31}P NMR (CD_3OD, 121 MHz): δ = 22.77; ES$^+$ MS ($C_{26}H_{21}ONP$)Cl (429) *m*/*z* 394 (100) $[M]^+$; HRMS (ES$^+$) $[M]^+$ calcd for $C_{26}H_{21}ONP$: 394.1355, found: 394.1358

4.2. *N*-Methyl-*N*-(2-tosyloxyethyl)-4-aminobenzaldehyde (15)

A solution of *N*-methyl-*N*-(2-hydroxyethyl)-4-aminobenzaldehyde (**14**) (1.00 g, 5.6 mmol) and Et_3N (1.15 mL, 7.3 mmol) in dichloromethane (50 mL) was stirred for 10 min at rt. Thereafter, *p*-toluenesulfonyl chloride (1.6 g, 8.4 mmol) was added and the reaction mixture was stirred for more 16 h. Then, the reaction mixture was extracted with sat. sol. $NaHCO_3$ (50 mL). The organic phase was dried over $MgSO_4$, filtered and the filtrate was concentrated by vacuum evaporation. Column chromatography on silica gel (*n*-hexane/EtOAc 2:1) gave **15** (1.34 g, 73%) as a light yellow solid—R_f = 0.58 (*n*-hexane/EtOAc 1:1); ^{1}H NMR ($CDCl_3$, 300 MHz): δ = 2.36 (s, CH_3, 3H), 2.97 (s, NCH_3, 3H), 3.69 (t, J = 5.7 Hz, OCH_2, 2H) 4.17 (t, J = 5.7 Hz, NCH_2, 2H), 6.55 (d, ^3J = 8.7 Hz, 1H), 7.20 (d, ^3J = 8.7 Hz, 1H), 7.64 (d, ^3J = 8.7 Hz, 2H), 9.71 (s, CHO, 1H); ^{13}C NMR ($CDCl_3$, 75 MHz): δ = 21.59, 39.23, 50.84, 66.44, 111.06 (2C), 125.87, 127.73 (2C), 129.81 (2C), 131.91 (2C), 132.39, 145.09, 152.61, 190.20; ES$^+$ MS $C_{17}H_{19}O_4NS$ (333.04) *m*/*z* 334.2 (5) $[M+H]^+$; HRMS (ES$^+$) $[M+H]^+$ calcd for $C_{18}H_{20}O_4NS$: 334.1108, found: 334.1104.

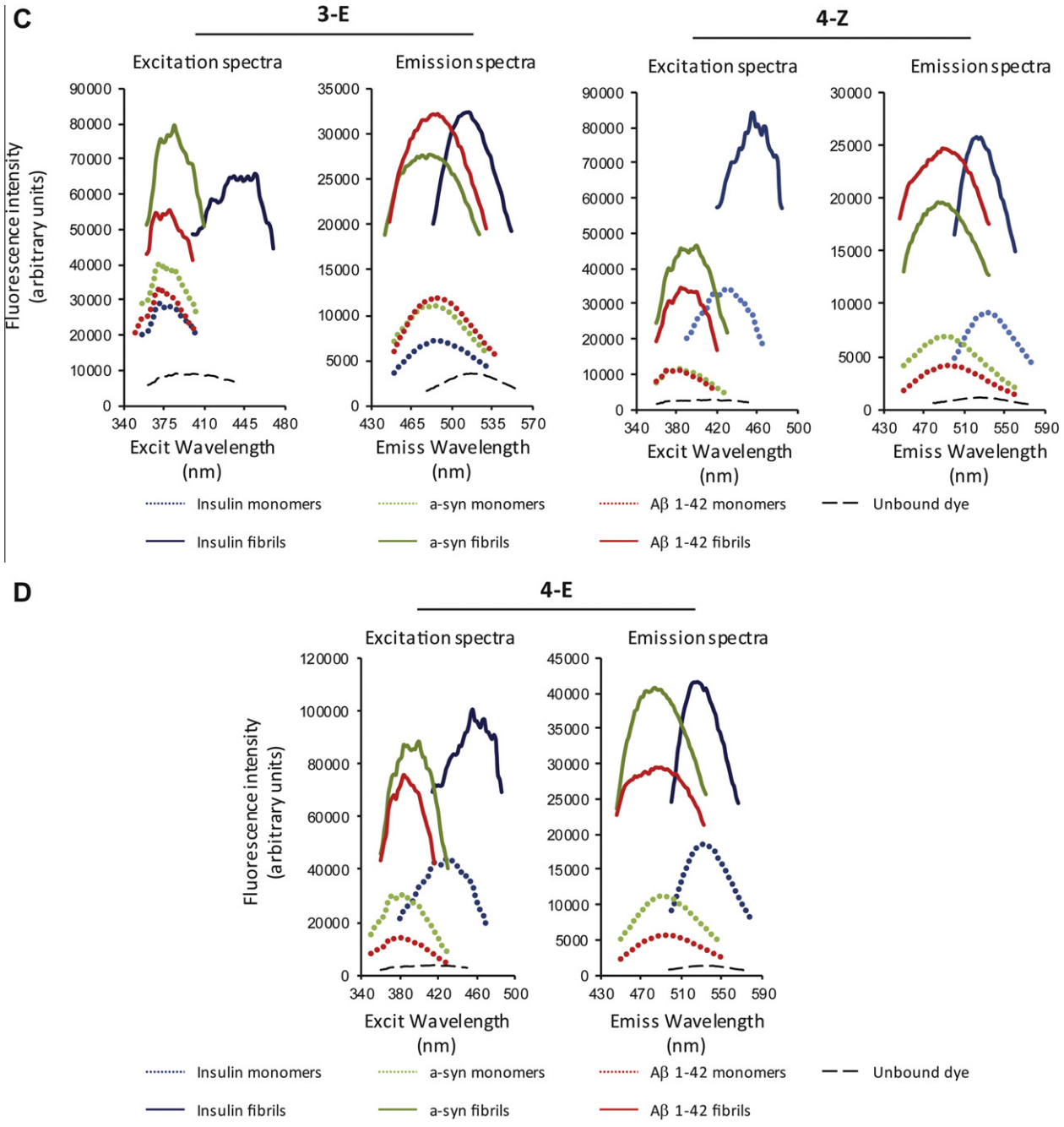

Fig. 4 (*continued*)

Table 2
Fluorescence intensity fold increase of *E*/*Z* isomers (2.25 μM) in the presence of 3.5 μM of fibrillary insulin, α-syn and Aβ(1–42) in comparison to the corresponding equimolar monomeric specie

	Insulin	a-syn	Ab(1–42)
1-*Z*	9.48 ± 0.53	2.98 ± 0.17	11.30 ± 1.40
1-*E*	4.48 ± 0.49	3.30 ± 0.23	7.41 ± 0.50
2-*Z*	1.63 ± 0.17	1.60 ± 0.22	1.28 ± 0.15
2-*E*	1.98 ± 0.25	1.98 ± 0.13	2.69 ± 0.29
3-*E*	4.50 ± 0.36	2.49 ± 0.16	2.71 ± 0.18
4-*Z*	2.84 ± 0.12	2.84 ± 0.11	5.9 ± 0.57
4-*E*	2.23 ± 0.15	3.63 ± 0.21	5.17 ± 0.27

4.3. *N*-Methyl-*N*-((2'-*O*-*tert*-butylcarbonate)ethyl)-4-aminobenzaldehyde (16)

A solution of *N*-Methyl-*N*-(2-hydroxyethyl)-4-aminobenzaldehyde (**14**) (1.0 g, 5–6 mmol), di-*tert*-butyl-dicarbonate (2.0 g, 9.2 mmol) and DMAP (33 mg, 0.3 mmol) in THF (30 mL) was stirred at room temperature for 2 h. Then, MeOH (50 mL) was added and the reaction mixture was stirred for 30 min more. Thereafter, the solvent was removed and the residue was submitted to column chromatography on silica gel (*n*-hexane/EtOAc 1:1) to give **16** (1.5 g, 95%)—R_f = 0.85 (*n*-hexane/EtOAc 1:1); ^{1}H NMR ($CDCl_3$, 300 MHz): δ = 1.39 (s, 9H), 3.05 (s, 3H), 3.67 (t, J = 6.0 Hz, 2H), 4.22 (t, J = 6.0 Hz, 2H), 6.71 (d, ^3J = 8.8 Hz, 2H), 7.68 (d, ^3J = 8.8 Hz, 2H), 9.70 (s, 1H); ^{13}C NMR ($CDCl_3$, 75 MHz): δ = 27.39 (3C), 38.55, 50.47, 63.06, 82.16, 110.67, 110.86, 125.42, 131.78 (2C), 153.03, 153.11, 189.90; ES$^+$ MS $C_{15}H_{21}NO_4$ (279) m/z 302.1 (100) [M+Na]$^+$.

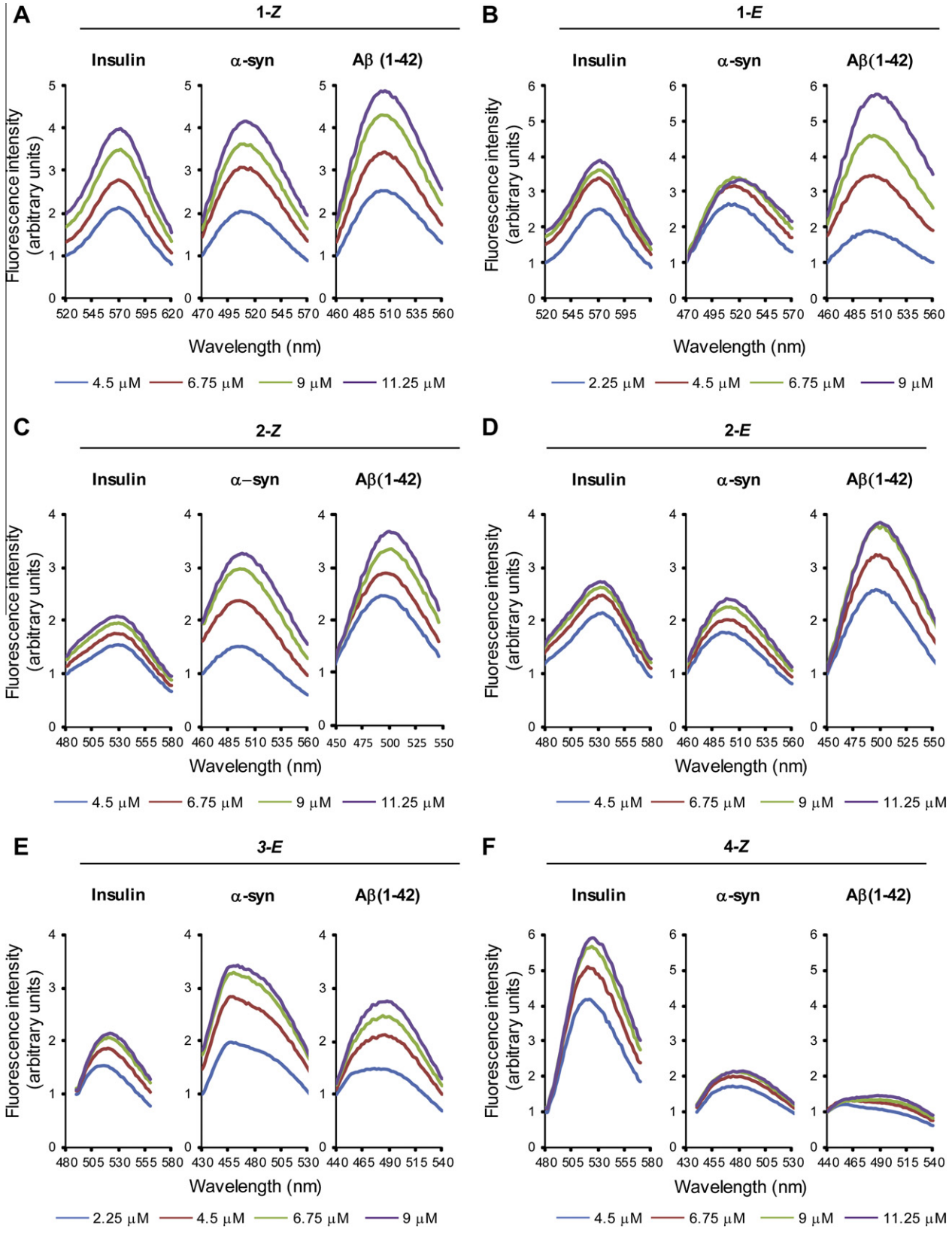

Figure 5. Fluorescence intensity binding assays in the presence of α-syn, insulin and Aβ(1–42) fibrillar species (7 μM) with varying concentrations of (A) **1**-*Z* (4.5–11.25 μM), (B) **1**-*E* (2.25–9 μM), (C) **2**-*Z* (4.5–11.25 μM), (D) **2**-*E* (4.5–11.25 μM), (E) **3**-*E* (2.25 and 9 μM), (F) **4**-*Z* (4.5–11.25 μM) and (G) **4**-*E* (2.25 and 9 μM) in 50 mM Tris–HCl buffer pH 7.4. All spectra were recorded at fixed maximum emission and excitation wavelengths for the different species according to Table 1.

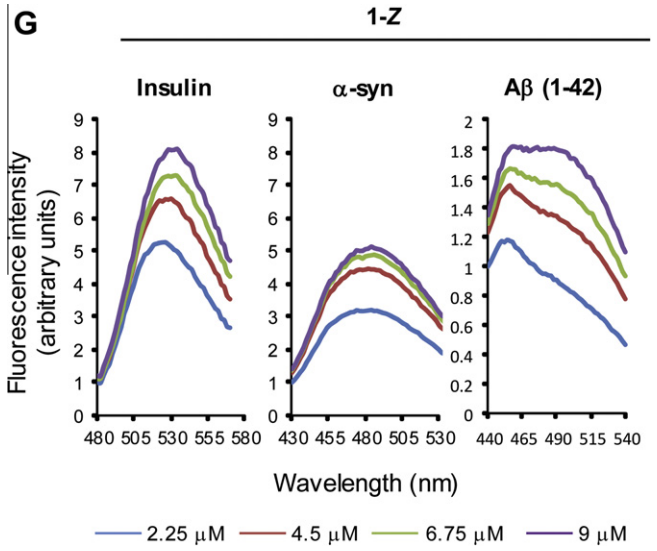

Fig. 5 (*continued*)

4.4. 2-[*N*-methyl-*N*-(2'-tosyloxyethyl)-4'-aminostyryl]benzothiazole (19)

To a stirred solution of **11** (1.57 g, 3.5 mmol) in benzene (25 mL) was added K^{t}BuO (400 mg, 3.6 mmol) at rt. After 3 h, the reaction mixture was diluted with EtOAc (100 mL) and was extracted with water (100 mL). The organic phase was dried over $MgSO_4$, filtered and the filtrate was dried under vacuum. Then, the resulting phosphorane (**17**) and **6** (450 mg, 1.4 mmol) were dissolved in anhydrous THF (24 mL) and refluxed overnight. Thereafter, the solvent was concentrated and the reaction crude was re-dissolved in CH_2Cl_2 (100 mL). The organic phase was extracted with sat. sol. of $NaHCO_3$ (100 mL). The organic extract was dried over $MgSO_4$, filtered and the filtrate was concentrated. The crude product was submitted to column chromatography on silica gel (*n*-hexane/EtOAc 2:1) to give a mixture of **19**-*Z* and **19**-*E* (580 mg, 89%)

4.4.1. *Z*-2-[*N*-methyl-*N*-(2'-tosyloxyethyl)-4'-aminostyryl]benzothiazole (19-*Z*)

R_f = 0.66 (*n*-hexane/EtOAc 1:1); ^{1}H NMR ($CDCl_3$, 300 MHz): δ = 2.37 (s, CH_3, 3H), 2.92 (s, NCH_3, 3H), 3.65 (t, J = 5.7 Hz, 2H), 4.18 (t, J = 5.7 Hz, 2H), 6.53 (d, ^3J = 8.5 Hz, 2H), 6.72 (d, ^ZJ = 12.3 Hz, 1H), 6.93 (d, ^ZJ = 12.3 Hz, 1H), 7.25–7.44 (m, 6H), 7.70 (d, ^3J = 8.5 Hz, 2H), 7.73 (d, ^3J = 8.1 Hz, 1H), 7.97 (d, ^3J = 8.1 Hz, 1H); ^{13}C NMR ($CDCl_3$, 75 MHz): δ = 21.65, 38.96, 51.00, 66.79, 111.52, 120.85, 121.30, 122.72, 123.77, 125.17, 125.99, 127.83, 129.83, 130.85, 132.60, 137.95, 144.95, 148.55; ES$^+$ MS $C_{25}H_{24}N_2O_3S_2$ (464.60) *m*/*z* 487.2 (100) [M+Na]$^+$; HRMS (ES$^+$) [M+H]$^+$ calcd for $C_{25}H_{25}O_3N_2S_2$: 465.1301, found: 465.1295.

4.4.2. *E*-2-[*N*-methyl-*N*-(2'-tosyloxyethyl)-4'-aminostyryl]benzothiazole (19-*E*)

R_f = 0.72 (*n*-hexane/EtOAc 1:1); ^{1}H NMR ($CDCl_3$, 300 MHz): δ = 2.37 (s, CH_3, 3H), 2.93 (s, NCH_3, 3H), 3.65 (t, J = 5.7 Hz, 2H), 4.18 (t, J = 5.7 Hz, 2H), 6.54 (d, ^3J = 8.7 Hz, 2H), 7.18 (d, ^EJ = 16.2 Hz, 1H), 7.30–7.45 (m, 7H), 7.67 (d, ^3J = 8.7 Hz, 2H), 7.81 (d, ^3J = 7.6 Hz, 1H), 7.93 (d, ^3J = 7.6 Hz, 1H); ^{13}C NMR ($CDCl_3$, 75 MHz): δ = 21.69, 39.12, 50.97, 66.96, 111.89, 117.47, 121.40, 122.35, 123.88, 124.92, 126.24, 127.80, 129.01, 129.81, 132.49, 138.13, 145.00, 149.07; ES$^+$ MS $C_{25}H_{24}N_2O_3S_2$ (464.60) *m*/*z* 487.2 (100) [M+Na]$^+$; HRMS (ES$^+$) [M+H]$^+$ calcd for $C_{25}H_{25}N_2O_3S_2$: 465.1301, found: 465.1295.

4.5. 2-[*N*-methyl-*N*-(2'-tosyloxyethyl)-4'-aminostyryl]benzoxazole (20)

Compound **20** was prepared as described above for compound **19**, starting from **12** (2.0 g, 4.6 mmol). Its purification was carried out by column chromatography on silica gel (*n*-hexane/$CHCl_3$/EtOAc 3:1:1) to give the mixture of **20**-*Z* and **20**-*E* (550 mg, 65%).

4.5.1. *Z*-2-[*N*-methyl-*N*-(2'-tosyloxyethyl)-4'-aminostyryl]benzoxazole (20-*Z*)

R_f = 0.52 (*n*-hexane/$CHCl_3$/EtOAc 3:1:1); ^{1}H NMR ($CDCl_3$, 300 MHz): δ = 2.35 (s, 3H), 2.95 (s, 3H), 3.66 (t, J = 6.0 Hz, 2H), 4.18 (t, J = 6.0 Hz, 2H), 6.29 (d, $^3J^Z$ = 13.0 Hz, 1H), 6.55 (d, ^3J = 9.0 Hz, 2H), 6.85 (d, $^3J^Z$ = 13.0 Hz, 1H), 7.23 (d, ^3J = 7.2 Hz, 2H), 7.28–7.31 (m, 2H), 7.43–7.46 (m, 1H), 7.67–7.72 (m, 3H), 7.82 (d, ^3J = 9.0 Hz, 2H); ^{13}C NMR ($CDCl_3$, 75 MHz): δ = 21.59, 39.06, 50.97, 66.79, 109.60, 110.28, 111.11 (2C), 111.89, 119.78, 124.29, 124.94, 127.81 (2C), 129.83 (2C), 132.18 (2C), 132.61, 139.81, 142.11, 144.96, 148.82, 149.92, 162.42; ES$^+$ MS $C_{25}H_{24}N_2O_4S$ (448.53) *m*/*z* 471 (100) [M+Na]$^+$; HRMS (ES$^+$) [M+Na]$^+$ calcd for $C_{25}H_{24}N_2O_4NaS$: 471.1347, found: 471.1336.

4.5.2. *E*-2-[*N*-methyl-*N*-(2'-tosyloxyethyl)-4'-aminostyryl]benzoxazole (20-*E*)

R_f = 0.30 (*n*-hexane/$CHCl_3$/EtOAc 3:1:1); ^{1}H NMR ($CDCl_3$, 300 MHz): δ = 2.38 (s, 3H), 2.94 (s, 3H), 3.66 (t, J = 6.0 Hz, 2H), 4.18 (t, J = 6.0 Hz, 2H), 6.55 (d, ^3J = 8.7 Hz, 2H), 6.83 (d, $^3J^E$ = 16.5 Hz, 1H), 7.21–7.29 (m, 4H), 7.40 (d, ^3J = 8.7 Hz, 2H), 7.46–7.49 (m, 1H), 8.64–7.71 (m, 4H); ^{13}C NMR ($CDCl_3$, 75 MHz): δ = 21.76, 39.14, 50.98, 66.65, 108.89, 110.12, 111.87 (2C), 119.32, 123.72, 124.38, 124.68, 127.80 (2C), 129.24 (2C), 129.81 (2C), 132.53, 139.86, 142.06, 139.86, 142.06, 145.00, 149.34, 150.29, 163.78; ES$^+$ MS $C_{25}H_{24}N_2O_4S$ (448.53) *m*/*z* 471 (100) [M+Na]$^+$; HRMS (ES$^+$) [M+Na]$^+$ calcd for $C_{25}H_{24}N_2O_4$: NaS 471.1347, found: 471.1336.

4.6. 2-[*N*-methyl-*N*-(2'-*O*-*tert*-butylcarbonatethyl)-4'-aminostyryl]benzimidazole (21)

To a solution of phosphonium salt **13** (3.4 g, 7.8 mmol) and **16** (860 mg, 3.1 mmol) in anhydrous methanol (32 mL) was added NaOMe (300 mg, 2.7 mmol) at rt under a nitrogen atmosphere. Then, the reaction mixture was stirred at 50 °C overnight. At the end of the reaction, the solvent was removed under vacuum and the crude was taken upon CH_2Cl_2 (100 mL). The organic phase was washed with a sat. sol. of $NaHCO_3$ (100 mL), dried over Na_2SO_4, filtered and the filtrate was concentrated. The residue was submitted to column chromatography on silica gel (*n*-hexane/EtOAc 2:1) to give the mixture of **21**-*Z* and **21**-*E* (810 mg, 67%)

Table 3
Amyloid binding constants (μM^{-1}) towards aggregates of insulin, α-syn and Aβ(1–42) for *E* and *Z* geometric isomers of compounds **1**–**4** and ThT

	1-*Z*	**1**-*E*	**2**-*Z*	**2**-*E*	**3**-*E*	**4**-*Z*	**4**-*E*	ThT
Insulin	8.59 ± 0.58	1.79 ± 0.46	3.24 ± 0.16	2.28 ± 0.20	1.54 ± 0.15	3.86 ± 0.36	1.22 ± 0.24	2.54 ± 0.39
α-syn	7.35 ± 0.42	1.38 ± 0.33	7.43 ± 0.29	3.24 ± 0.16	3.31 ± 0.34	1.85 ± 0.24	1.81 ± 0.31	11.93 ± 0.94
Aβ (1–42)	23.96 ± 3.57	10.67 ± 1.55	5.99 ± 0.56	4.48 ± 0.38	3.63 ± 0.18	3.52 ± 0.17	5.19 ± 0.57	2.56 ± 0.29

4.6.1. *Z*-2-[*N*-methyl-*N*-(2'-O-tert-butylcarbonatethyl)-4'-aminostyryl]benzimidazole (21-*Z*)

R_f = 0.54 (*n*-hexane/EtOAc 2:1); ^{1}H NMR ($CDCl_3$, 300 MHz): δ = 1.45 (s, 9H), 3.02 (s, 3H), 3.65 (t, *J* = 6.0 Hz, 2H), 4.25 (t, *J* = 6.0 Hz, 2H), 6.55 (d, $^3J^Z$ = 12.3 Hz, 1H), 6.70 (d, ^3J = 8.4 Hz, 2H), 6.89 (d, $^3J^Z$ = 12.3 Hz, 1H), 7.18–7.22 (m, 4H), 7.35 (d, ^3J = 8.4 Hz, 2H); ^{13}C NMR ($CDCl_3$, 75 MHz): δ = 27.68 (3C), 38.68, 50.87, 63.46, 82.37, 111.95 (2C), 116.88, 123.91, 129.93 (2C), 135.61, 148.95, 150.05, 153.33; ES$^+$ MS $C_{23}H_{27}N_3O_3$ (393) *m*/*z* 394.2 (100) [M+H]$^+$; HRMS (ES$^+$) [M+H]$^+$ calcd for $C_{23}H_{28}N_3O_3$: 394.2125 found: 394.2126.

4.6.2. *E*-2-[*N*-methyl-*N*-(2'-O-tert-butylcarbonatethyl)-4'-aminostyryl]benzimidazole (21-*E*)

R_f = 0.42 (*n*-hexane/EtOAc 2:1); ^{1}H NMR ($CDCl_3$, 300 MHz): δ = 1.45 (s, 9H), 2.96 (s, 3H), 3.59 (t, *J* = 6.0 Hz, 2H), 4.19 (t, *J* = 6.0 Hz, 2H), 6.58 (d, ^3J = 8.4 Hz, 2H), 6.99 (dd, ^4J = Hz, $^3J^E$ = 16.5 Hz, 1H), 7.21–7.28 (m, 4H), 7.59–7.64 (m, 3H); ^{13}C NMR ($CDCl_3$, 75 MHz): δ = 27.65 (3C), 38.60, 50.75, 63.51, 82.35, 111.83 (2C), 111.87 (2C), 122.47, 124.02, 128.57 (2C), 135.90, 149.32, 152.43, 153.33; ES$^+$ MS $C_{23}H_{27}N_3O_3$ (393) *m*/*z* 394.2 (100) [M+H]$^+$; HRMS (ES$^+$) [M+H]$^+$ calcd for $C_{23}H_{28}N_3O_3$: 394.2125 found: 394.2126.

4.7. *E*-2-[*N*-methyl-*N*-(2'-tosyloxyethyl)-4'-aminostyryl]benzimidazole (22-*E*)

A solution of **21**-*E*/**21**-*Z* (810 mg, 2.1 mmol) in CH_2Cl_2 (12 mL) was stirred with TFA (6 mL) at rt for 90 min. Then, the solvent was removed under vaccum. The resulting crude was re-dissolved in CH_2Cl_2 (50 mL) and was reacted with Et_3N (0.4 mL) and *p*-TsCl (500 mg, 2.6 mmol) for 30 min. Thereafter, the reaction mixture was diluted with CH_2Cl_2 (100 mL) and was washed with a sat. sol. of $NaHCO_3$ (100 mL). The organic phase was dried over Na_2SO_4, was filtered and the filtrate was evaporated. The residue was submitted to column chromatography on silica gel (*n*-hexane/EtOAc 1:2) to give **22**-*E* (295 mg, 32%)—R_f = 0.19 (*n*-hexane/EtOAc 1:1); ^{1}H NMR ($CDCl_3$, 300 MHz): δ = 2.31 (s, 3H), 3.06 (s, 3H), 3.56 (t, *J* = 5.4 Hz, 2H), 3.85 (t, *J* = 5.4 Hz, 2H), 6.78 (d, ^3J = 8.7 Hz, 2H), 7.18 (d, ^3J = 7.9 Hz, 2H), 7.28–7.30 (m, 2H), 7.53 (d, ^3J = 8.7 Hz, 2H), 7.60–7.63 (m, 1H), 7.67 (d, $^3J^E$ = 15.6 Hz, 1H), 7.75 (d, ^3J = 7.9 Hz, 2H), 7.83 (d, $^3J^E$ = 15.6 Hz, 1H), 8.02–8.05 (m, 1H); ^{13}C NMR ($CDCl_3$, 75 MHz): δ = 21.60, 38.97, 54.70, 60.27, 109.29, 112.25 (2C), 113.86, 119.37, 124.34, 124.41, 125.09, 126.81 (2C), 129.43 (2C), 130.07 (2C), 133.08, 135.41, 140.15, 142.90, 145.68, 150.69, 152.31; ES$^+$ MS $C_{25}H_{25}O_3N_3$ (447) *m*/*z* 470.22 (95) [M+Na]$^+$; HRMS (ES$^+$) [M+H]$^+$ calcd for $C_{25}H_{26}N_3O_3S$: 448.1689, found: 448.1691.

4.8. *E*/*Z*-1-Methyl-2-[*N*-methyl-*N*-(2'-*O*-tert-butylcarbonatethyl)-4'-aminostyryl]benzimidazole (23)

To a solution of NaOH (535 mg, 13.4 mmol) in water (0.75 mL) were added **21**-*Z*/**21**-*E* (715 mg, 1.8 mmol), acetone (7.5 mL) and methyl iodide (145 μL, 2.3 mmol), dropwise with the flask cooling in ice water. The reaction mixture was stirred for 1 h at rt. Then, acetone was evaporated, the reaction mixture was diluted with water (100 mL) and was extracted with CH_2Cl_2 (100 mL). The organic phase was dried over Na_2SO_4, filtered and the filtrate was concentrated under vacuum to give the mixture of **23**-*Z* and **23**-*E* (710 mg, 96%)—R_f = 0.60 (*n*-hexane/EtOAc 2:1); ^{1}H NMR ($CDCl_3$, 300 MHz): δ = 1.41 (s, 9H), 1.42 (s, 9H), 2.91 (s, 3H), 3.00 (s, 3H), 3.41 (s, 3H), 3.54 (t, *J* = 6.0 Hz, 2H), 3.62 (t, *J* = 6.0 Hz, 2H), 3.77 (s, 3H), 4.13 (t, *J* = 6.0 Hz, 2H), 4.21 (t, *J* = 6.0 Hz, 2H), 6.32 (d, $^3J^Z$ = 12.3 Hz, 1H), 6.49 (d, ^3J = 9.0 Hz, 2H), 6.59 (d, ^3J = 9.0 Hz, 2H), 6.83 (d, $^3J^E$ = 15.6 Hz, 1H), 6.87 (d, $^3J^Z$ = 12.3 Hz, 1H), 7.10 (d, ^3J = 9.0 Hz, 2H), 7.13–7.26 (m, 6H), 7.47 (d, ^3J = 9.0 Hz, 2H), 7.69–7.72 (m, 1H), 7.74–7.77 (m, 1H), 7.86 (d, $^3J^E$ = 15.6 Hz, 1H); ^{13}C NMR ($CDCl_3$, 75 MHz): δ = 27.62 (3C), 38.62, 50.74, 63.40, 82.31, 107.97, 108.82, 109.33, 111.47, 111.79 (2C), 112.40, 118.78, 119.48, 121.86, 122.23, 124.34, 128.75 (2C), 130.31, 135.93, 137.43, 137.99, 143.16, 149.41, 152.11, 153.28; ES$^+$ MS $C_{24}H_{29}N_3O_3$ (407) *m*/*z* 430.2 (60) [M+Na]$^+$; HRMS (ES$^+$) [M+H]$^+$ calcd for $C_{24}H_{30}N_3O_3$: 408.2282, found; 408.2282.

4.9. 1-Methyl-2-[*N*-methyl-*N*-(2'-tosyloxyethyl)-4'-aminostyryl]benzimidazole (24)

Compound **24** was prepared as described above for compound **22**, starting from **21**-*Z*/**21**-*E* (680 mg, 1.7 mmol). Its purification was carried out by column chromatography on silica gel (*n*-hexane/EtOAc 1:1) to give the mixture of **24**-*Z* and **24**-*E* (540 mg, 69%).

4.9.1. *Z*-1-Methyl-2-[*N*-methyl-*N*-(2'-tosyloxyethyl)-4'-aminostyryl]benzimidazole (24-*Z*)

R_f = 0.38 (*n*-hexane/EtOAc 2:1); ^{1}H NMR ($CDCl_3$, 300 MHz): δ = 2.35 (s, 3H), 2.83 (s, 3H), 3.43 (s, 3H), 3.54 (t, *J* = 6.0 Hz, 2H), 4.17 (t, *J* = 6.0 Hz, 2H), 6.34 (m, 3H), 6.87 (d, $^3J^Z$ = 12.0 Hz, 1H), 7.07 (d, ^3J = 8.7 Hz, 2H), 7.18–7.30 (m, 4H), 7.64 (d, ^3J = 9.0 Hz, 2H), 7.70–7.75 (m, 2H); ^{13}C NMR ($CDCl_3$, 75 MHz): δ = 21.56, 30.26, 38.79, 50.81, 66.77, 109.39, 111.48 (2C), 112.67, 119.51, 122.01, 122.34, 124.36, 128.85 (2C), 130.35 (2C), 132.56 (2C), 135.33, 137.88, 143.26, 144.94, 148.22, 151.45; ES$^+$ MS $C_{26}H_{27}N_3O_3S$ (461) *m*/*z* 462.2 (100) [M+H]$^+$; HRMS (ES$^+$) [M+H]$^+$ calcd for $C_{26}H_{27}N_3O_3S$: 462.1846; found: 462.1834.

4.9.2. *E*-1-Methyl-2-[*N*-methyl-*N*-(2'-tosyloxyethyl)-4'-aminostyryl]benzimidazole (24-*E*)

R_f = 0.18(*n*-hexane/EtOAc 2:1); ^{1}H NMR ($CDCl_3$, 300 MHz): δ = 2.37 (s, 3H), 2.92 (s, 3H), 3.64 (t, *J* = 6.0 Hz, 2H), 3.82 (s, 3H), 4.17 (t, *J* = 6.0 Hz, 2H), 6.54 (d, ^3J = 8.4 Hz, 2H), 6.86 (d, $^3J^E$ = 15.9 Hz, 1H), 7.18–7.30 (m, 4H), 7.43 (d, ^3J = 8.4 Hz, 2H), 7.67 (d, ^3J = 8.7 Hz, 2H), 7.70–7.75 (m, 2H), 7.86 (d, $^3J^E$ = 15.9 Hz, 1H); ^{13}C NMR ($CDCl_3$, 75 MHz): δ = 21.62, 29.63, 38.97, 50.96, 66.77, 108.30, 108.91, 111.84 (2C), 118.81, 122.01, 122.34, 124.67, 127.75 (2C), 128.71 (2C), 129.78 (2C), 135.95, 137.36, 140.09, 144.94, 148.78, 152.01; ES$^+$ MS $C_{26}H_{27}N_3O_3S$ (461) *m*/*z* 462.2 (100) [M+H]$^+$; HRMS (ES$^+$) [M+H]$^+$ calcd for $C_{26}H_{27}N_3O_3S$: 462.1846; found: 462.1834.

4.10. 2-[*N*-methyl-*N*-(2'-fluoroethyl)-4'-aminostyryl]benzothiazole (1)

To a solution of **19**-*Z*/**19**-*E* (210 mg, 0.45 mmol) in anhydrous THF (23 mL) was added anhydrous TBAF (1.8 mL, 1.8 mmol, 1.0 M in THF). The reaction mixture was refluxed for 30 min. Thereafter the solvent was removed under vacuum; chloroform (50 mL) was added to the residue and was washed with sat sol $NaHCO_3$ (50 mL). The organic phase was dried over $MgSO_4$, filtered and the filtrate was concentrated. Column chromatography on silica gel (*n*-hexane/EtOAc 5:1) gave the mixture of **1**-*Z* and **1**-*E* (104 mg, 74%).

4.10.1. *Z*-2-[*N*-methyl-*N*-(2'-fluoroethyl)-4'-aminostyryl]benzothiazole (1-*Z*)

R_f = 0.36 (*n*-hexane/EtOAc 4:1); log*P*(o/w) = 4.83; ^{1}H NMR ($CDCl_3$, 300 MHz): δ = 3.05 (s, 3H, CH_3), 3.68 (dt, $J_{H,H}$ = 5.1 Hz, $J_{H,F}$ = 24.3 Hz, 2H), 4.61 (dt, $J_{H,H}$ = 5.1 Hz, $J_{H,F}$ = 47.4 Hz, 2H), 6.67 (d, ^3J = 8.7 Hz, 2H), 6.72 (d, $^Z J$ = 12 Hz, 1H), 6.95 (d, $^Z J$ = 12 Hz, 1H), 7.28 (ddd, ^4J = 1.2 Hz, ^3J = 7.2 Hz, ^3J = 7.8 Hz, 1H), 7.41 (ddd, ^4J = 1.2 Hz, ^3J = 7.2 Hz, ^3J = 8.1 Hz, 1H), 7.47 (d, ^3J = 8.7 Hz, 2H), 7.72 (ddd, ^5J = 0.4 Hz, ^4J = 1.2 Hz, ^3J = 7.8 Hz, 1H), 7.98 (ddd, ^5J = 0.4 Hz ^4J = 1.2 Hz, ^3J = 8.1 Hz, 1H); ^{13}C NMR ($CDCl_3$, 75 MHz):

δ = 39.07, 52.45 (d, $J_{C,F}$ = 20.8 Hz), 81.72 (d, $J_{C,F}$ = 168.6 Hz), 111.68 (2C), 120.87, 121.25, 122.78, 123.65, 125.07, 125.89, 130.89 (2C), 135.10, 137.95, 149.18, 152.84, 165.27, ^{19}F ($CDCl_3$, 282 MHz): δ = −223.09 (m); ES$^+$ MS $C_{18}H_{17}N_2FS$ (312.11) *m*/*z* 313.2 (100) $[M+H]^+$; HRMS (ES$^+$) $[M+H]^+$ calcd for $C_{18}H_{18}N_2FS$: 313.1169, found: 313.1167.

4.10.2. *E*-2-[*N*-methyl-*N*-(2'-fluoroethyl)-4'-amino styryl]benzo thiazole (1-*E*)

R_f = 0.24 (*n*-hexane/EtOAc 4:1); log*P*(o/w) = 4.83; ^{1}H NMR ($CDCl_3$, 300 MHz): δ = 3.06 (s, 3H, CH_3), 3.69 (dt, $J_{H,H}$ = 5.1 Hz, $^3J_{H,F}$ = 24.6 Hz, 2H), 4.60 (dt, $J_{H,H}$ = 5.1 Hz, $^2J_{H,F}$ = 47.1 Hz, 2H), 6.70 (d, ^3J = 9.0 Hz, 2H), 7.19 (d, ^EJ = 16.2 Hz, 1H), 7.31 (ddd, ^4J = 1.2 Hz, ^3J = 7.6 Hz, ^3J = 7.8 Hz, 1H), 7.39–7.47 (m, 3H), 7.80 (d, ^3J = 7.8 Hz, 1H), 7.92 (d, ^3J = 8.1 Hz, 1H); ^{13}C NMR ($CDCl_3$, 75 MHz): δ = 39.12, 52.37 (d, $J_{C,F}$ = 21.45 Hz), 81.66 (d, $J_{C,F}$ = 169.2 Hz), 112.03 (2C), 117.57, 121.36, 122.41, 123.80, 124.81, 126.12, 129.05 (2C), 134.06, 138.09, 149.71, 153.85, 168.10; ^{19}F ($CDCl_3$, 282 MHz): δ = −223.15 (m); ES$^+$ MS $C_{18}H_{17}N_2FS$ (312.11) *m*/*z* 313.2 (100) $[M+H]^+$; HRMS (ES$^+$) $[M+H]^+$ calcd for $C_{18}H_{18}N_2FS$: 313.1169, found: 313.1167.

4.11. 2-[*N*-methyl-*N*-(2'-fluoroethyl)-4'-amino styryl]benzo xazole (2)

Compound **2** was prepared as described above for compound **1**, starting from **20**-*Z*/**20**-*E* (250 mg, 0.55 mmol). Its purification was carried out by column chromatography on silica gel (*n*-hexane/EtOAc 4:1) to give the mixture of **2**-*Z* and **2**-*E* (124 mg, 76%).

4.11.1. *Z*-2-[*N*-methyl-*N*-(2'-fluoroethyl)-4'-amino styryl]benzo xazole (2-*Z*)

R_f = 0.52 (*n*-hexane/EtOAc 4:1); log*P*(o/w) = 4.01; ^{1}H NMR ($CDCl_3$, 300 MHz): δ = 3.07 (s, 3H), 3.70 (dt, $J_{H,H}$ = 5.1 Hz, $^3J_{H,F}$ = 24.3 Hz, 2H), 4.61 (dt, $J_{H,H}$ = 5.1 Hz, $^2J_{H,F}$ = 47.2 Hz, 2H), 6.28 (d, $^3J^Z$ = 12.9 Hz, 1H), 6.70 (d, ^3J = 8.4 Hz, 2H), 6.87 (d, $^3J^Z$ = 12.9 Hz, 1H), 7.27–7.32 (m, 2H), 7.43–7.46 (m, 1H), 7.69–7.72 (m, 1H), 7.88 (d, ^3J = 8.4 Hz, 2H); ^{13}C NMR ($CDCl_3$, 75 MHz): δ = 39.09, 52.31 (d, $J_{C,F}$ = 20.8 Hz), 81.69 (d, $J_{C,F}$ = 169.7 Hz), 109.43, 110.23, 111.23 (2C), 119.78, 123.81, 124.23, 124.85, 132.25 (2C), 139.91, 142.17, 149.49, 149.94, 162.52; ^{19}F ($CDCl_3$, 282 MHz): δ = −223.18 (m), ES$^+$ MS $C_{18}H_{17}ON_2F$ (296.13) *m*/*z* 297.2 (100) $[M+H]^+$; HRMS (ES$^+$) $[M+H]^+$ calcd for $C_{18}H_{18}ON_2F$: 297.1398, found: 297.1404.

4.11.2. *E*-2-[*N*-methyl-*N*-(2'-fluoroethyl)-4'-aminostyryl]benzo xazole (2-*E*)

R_f = 0.30 (*n*-hexane/EtOAc 4:1); log*P*(o/w) = 4.01; ^{1}H NMR ($CDCl_3$, 300 MHz): δ = 3.07 (s, 3H), 3.69 (dt, $J_{H,H}$ = 5.1 Hz, $^3J_{H,F}$ = 24.6 Hz, 2H), 4.61 (dt, $J_{H,H}$ = 5.1 Hz, $^2J_{H,F}$ = 47.1 Hz, 2H), 6.70 (d, ^3J = 8.7 Hz, 2H), 6.83 (d, $^3J^E$ = 16.2 Hz, 1H), 7.26–7.30 (m, 2H), 7.46–7.49 (m, 3H), 7.64–7.67 (m, 1H), 7.70 (d, $^3J^E$ = 16.2 Hz, 1H); ^{13}C NMR ($CDCl_3$, 75 MHz): δ = 39.11, 52.28 (d, $J_{C,F}$ = 20.8 Hz), 81.62 (d, $J_{C,F}$ = 169.7 Hz), 108.97, 110.06, 112.03 (2C), 119.37, 123.67, 124.27, 124.55, 129.27 (2C), 139.76, 142.36, 149.99, 150.35, 163.87; ^{19}F ($CDCl_3$, 282 MHz): δ = −223.17 (m); ES$^+$ MS $C_{18}H_{17}ON_2F$ (296.13) *m*/*z* 8) 297.2 (100) $[M+H]^+$; HRMS (ES$^+$) $[M+H]^+$ calcd for $C_{18}H_{18}ON_2F$: 297.1398, found: 297.1404

4.12. 2-[*N*-methyl-*N*-(2'-fluorethyl)-4'-aminostyryl]benzimi dazole (3)

Compound **3** was prepared as described above for compound **1**, starting from **22-*E*** (280 mg, 0.6 mmol). The organic extract was dried over Na_2SO_4. Its purification was carried out by column chromatography on silica gel (*n*-hexane/EtOAc 1:1) to give the mixture of **3**-*Z* and **3**-*E* (30 mg, 16%).

4.12.1. *Z*-2-[*N*-methyl-*N*-(2'-fluorethyl)-4'-aminostyryl]benzi midazole (3-*Z*)

R_f = 0.35 (*n*-hexane/EtOAc 1:1); log*P*(o/w) = 3.95; ^{1}H NMR ($CDCl_3$, 300 MHz): δ = 3.07 (s, 3H), 3.68 (dt, $J_{H,H}$ = 4.8 Hz, $J_{H,F}$ = 29.7 Hz, 2H), 4.62 (dt, $J_{H,H}$ = 4.8 Hz, $J_{H,F}$ = 47.1 Hz, 2H) 6.55 (d, $^3J^Z$ = 12.3 Hz, 1H), 6.70 (d, ^3J = 8.7 Hz, 2H), 6.89 (d, $^3J^Z$ = 12.3 Hz, 1H), 7.15–7.20 (m, 2H), 7.33 (d, ^3J = 8.7 Hz, 2H), 7.42–7.50 (m, 2H) ^{13}C NMR ($CDCl_3$, 75 MHz): δ = 38.90, 52.39 (d, $J_{C,F}$ = 20.9 Hz), 81.64 (d, $J_{C,F}$ = 169.2 Hz), 112.09 (2C), 116.99, 122.65 (2C), 123.99 (2C), 129.92 (2C), 135.56, 149.00, 149.97; ^{19}F ($CDCl_3$, 282 MHz): δ = δ = −223.00 (m); ES$^+$ MS $C_{18}H_{18}FN_3$ (295) *m*/*z* 296.2 (100) $[M+H]^+$; HRMS (ES$^+$) $[M+H]^+$ calcd for $C_{18}H_{19}N_3F$: 296.1558, found: 296.1562.

4.12.2. *E*-2-[*N*-methyl-*N*-(2'-fluorethyl)-4'-aminostyryl] benzimidazole (3-*E*)

R_f = 0.18 (*n*-hexane/EtOAc 1:1); log*P*(o/w) = 3.95; ^{1}H NMR ($CDCl_3$, 300 MHz): δ = 3.03 (s, 3H), 3.66 (dt, $J_{H,H}$ = 5.1 Hz, $J_{H,F}$ = 24.6 Hz, 2H), 4.58 (dt, $J_{H,H}$ = 5.1 Hz, $J_{H,F}$ = 47.1 Hz, 2H), 6.64 (d, ^3J = 8.7 Hz, 2H), 6.91 (d, $^3J^E$ = 16.5 Hz, 1H), 7.18–7.21 (m, 2), 7.37 (d, ^3J = 8.7 Hz, 2H), 7.48–7.60 (m, 3H); ^{13}C NMR ($CDCl_3$, 75 MHz): δ = 39.10, 52.40 (d, $J_{C,F}$ = 21.4 Hz), 81.67 (d, $J_{C,F}$ = 169.2 Hz), 111.94 (2C), 112.05 (2C), 122.61, 124.12 (2C), 128.55 (2C), 125.55, 149.43, 151.81; ^{19}F ($CDCl_3$, 282 MHz): δ = −223.04 (m); ES$^+$ MS $C_{18}H_{18}FN_3$ (295) *m*/*z* 296 (100) $[M+H]^+$; HRMS (ES$^+$) $[M+H]^+$ calcd for $C_{18}H_{19}N_3F$: 296.1558, found: 296.1562.

4.13. 1-Methyl-2-[*N*-methyl-*N*-(2'-fluorethyl)-4'-aminostyryl] benzimidazole (4)

Compound **4** was prepared as described above for compound **1**, starting from **24**-*Z*/**24**-*E* (300 mg, 0.6 mmol). The organic extract was dried over Na_2SO_4. Its purification was carried out by column chromatography on silica gel (*n*-hexane/EtOAc 2:1) to give the mixture of **4**-*Z* and **4**-*E* (160 mg, 80%).

4.13.1. *Z*-1-Methyl-2-[*N*-methyl-*N*-(2'-fluorethyl)-4'-amino styryl]benzimidazole (4-*Z*)

R_f = 0.29 (*n*-hexane/EtOAc 2:1); log*P*(o/w) = 4.34; ^{1}H NMR ($CDCl_3$, 300 MHz): δ = 2.95 (s, 3H), 3.45 (s, 3H), 3.57 (dt, $J_{H,H}$ = 5.1 Hz, $J_{H,F}$ = 24.3 Hz, 2H), 4.51 (dt, $J_{H,H}$ = 5.1 Hz, $J_{H,F}$ = 47.4 Hz, 2H), 6.33 (d, $^3J^Z$ = 12.3 Hz, 1H), 6.49 (d, ^3J = 8.7 Hz, 2H), 6.88 (d, $^3J^Z$ = 12.3 Hz, 1H), 7.13 (d, ^3J = 8.7 Hz, 2H), 7.24–7.26 (m, 3H), 7.75–7.78 (m, 1H); ^{13}C NMR ($CDCl_3$, 75 MHz): δ = 30.24, 38.88, 52.25 (d, $J_{C,F}$ = 20.8 Hz), 81.60 (d, $J_{C,F}$ = 169.12 Hz), 109.31, 111.62 (2C), 112.47, 119.49, 121.94, 122.26, 124.17, 130.37 (2C), 135.31, 137.97, 143.26, 148.84, 151.53; ^{19}F ($CDCl_3$, 282 MHz): δ = −223.03 (m); ES$^+$ MS $C_{19}H_{20}FN_3$ (309) *m*/*z* 310 (10) $[M+H]^+$; HRMS (ES$^+$) $[M+H]^+$ calcd for $C_{19}H_{21}N_3F$: 310.1714, found: 310.1717.

4.13.2. *E*-1-Methyl-2-[*N*-methyl-*N*-(2'-fluorethyl)-4'-amino styryl]benzimidazole (4-*E*)

R_f = 0.21 (*n*-hexane/EtOAc 2:1); log*P*(o/w) = 4.34; ^{1}H NMR ($CDCl_3$, 300 MHz): δ = 3.05 (s, 3H), 3.68 (dt, $J_{H,H}$ = 5.1 Hz, $J_{H,F}$ = 24.3 Hz, 2H), 3.81 (s, 3H), 4.60 (dt, $J_{H,H}$ = 5.1 Hz, $J_{H,F}$ = 47.1 Hz, 2H), 6.69 (d, ^3J = 9.0 Hz, 2H), 6.86 (d, $^3J^E$ = 15.6 Hz, 1H), 7.20–7.29 (m, 3H), 7.49 (d, ^3J = 9.0 Hz, 2H), 7.70–7.73 (m, 1H), 7.87 (d, $^3J^E$ = 15.6 Hz, 1H); ^{13}C NMR ($CDCl_3$, 75 MHz): δ = 29.67, 39.08, 52.43 (d, $J_{C,F}$ = 21.37 Hz), 81.68 (d, $J_{C,F}$ = 169.20 Hz), 108.28, 108.86, 112.04(2C), 118.93, 121.98, 121.32, 124.64, 128.81 (2C), 136.02, 137.48, 143.27, 149.47, 152.14; ^{19}F ($CDCl_3$, 282 MHz): δ = −223.02 (m); ES$^+$ MS $C_{19}H_{20}FN_3$ (309) *m*/*z* 310 (10) $[M+H]^+$; HRMS (ES$^+$) $[M+H]^+$ calcd for $C_{19}H_{21}N_3F$: 310.1714, found: 310.1717.

4.14. X- ray diffraction analysis

White crystals of compound **12** suitable for X-ray diffraction studies were obtained by diffusion of diethyl ether into a concentrated methanolic solution of **12**. The X-ray diffraction analysis of **12** was performed on a Bruker AXS APEX CCD area detector diffractometer, using graphite monochromated Mo K_α radiation (0.71073 Å). Empirical absorption correction was carried out using SADABS.[38] Data collection and data reduction were done with the SMART and SAINT programs.[39] The structures were solved by direct methods with SIR97[40] and refined by full-matrix least-squares analysis with SHELXL-97[41] using the WINGX.[42] All nonhydrogen atoms were refined anisotropically. The remaining hydrogen atoms were placed in calculated positions. Molecular graphics were prepared using ORTEP3.[43]

4.15. Crystallographic data

$(C_{26}H_{21}NOP)^+Cl^-$, M_r 429.86, triclinic, space group $p\bar{1}$, $Z = 2$, $D_{calc} = 1.299$ g/cm^3, $a = 9.7244$ (3) Å, $b = 10.8474(3)$ Å, $c = 12.6058(4)$ Å, $\alpha = 68.2390(10)°$, $\beta = 71.740(2)°$, $\gamma = 64.9080(10)°$, $v = 1098.98(6)$ Å^3, μ(MoKα) 0.264 cm^{-3}, $F(000) = 448$, $\lambda = 0.71073$ Å. Data were collected using a crystal of $0.40 \times 0.30 \times 0.20$ mm^3. A total number of 9047 of reflections were collected for $2.58° < \theta < 25.68°$ and $-11 <= h <= 11$, $-13 <= k <= 11$, $-15 <= l <= 15$. There were 4146 independent reflections and 3681 reflections with $I > 2\sigma(I)$ were used in the refinement. The final R indices were $[I > 2\sigma(I)]$ $R_1 = 0.0330$, $wR_2 = 0.0858$ and (all data) $R_1 = 0.0380$, $wR_2 = 0.0886$. The goodness-of-fit on F^2 was 1.072 and the largest difference peak and hole was 0.350 and −0.304 eÅ^{-3}.

The crystallographic data of **12** have been deposited with the Cambridge Crystallographic Data Center (CCDC 826044).

4.16. Expression and purification of human α-syn

The expression and purification procedure of human α-syn was adapted from the literature.[44] Briefly, *E. coli* BL21 codon plus RIL strain (Stratagene, Santa Clara, USA) was transformed with human α-syn PT7-7 construct (a kind gift from Hilal Lashuel, EPFL, Lausanne) and expression was induced for 3 h with D-thiogalactopyranoside (IPTG, Calbiochem, Darmstadt, Germany) at a final concentration of 0.3 mM. Cells were harvested and resuspended in hyperosmotic buffer (40% Sucrose, 30 mM Tris-HCl, 2 mM EDTA, pH 7.3). The pellet was placed in a hypotonic solution, vortexed and the 35% ammonium sulfate salt resultant precipitate discarded. The supernatant was further precipitated in 60% ammonium sulfate, and the resulting pellet was separated by ion-exchange chromatography (HiTrap Q sepharose, GE Healthcare, NJ, USA) in Tris–HCl 30 mM pH 7.3 buffer with a NaCl gradient. Resulting 15 KDa α-syn positive samples, as judged by 15% SDS–PAGE (Bio-Rad, Hercules, California, USA, according to the supplier's instructions) were collected and further purified by gel filtration chromatography (Superdex 200, Ge Healthcare, NJ, USA). SDS–PAGE, followed by western-blot analysis (using standard procedures), confirmed the monomeric purification of α-syn (Syn-1 BD Transduction Laboratories, CA, USA).

4.17. Polymerization of insulin, α-syn and Aβ 1–42 fibrils

Human insulin was prepared in Tris–HCl 50 mM at 3 mg mL^{-1}, pH 3. Purified α-syn was resuspended at 3 mg mL^{-1} in Tris–HCl 50 mM pH 7.4. Human Aβ-(1–42)-peptide (rPeptide, Leipzig, Germany) was prepared at 0.5 mg/ml in 1% ammonium hydroxide (Sigma) in Mili-Q type II water (Millipore, Billerica, MA, USA). Samples were incubated at 37 °C for 6 days in a thermomixer (Eppendorph, Hamburg, Germany) at 1400 rpm. Fibrils were collected after ultracentrifugation at 40,000*g* for 1 h at 4 °C and supernatant collected for protein quantification. To determine fibril concentrations, supernatant protein concentration was assayed and the difference between the starting and remaining supernatant concentration was assumed as that of the fibrils, an approximation that is widely used in the field. The formation of fibrils was confirmed by Thioflavin T binding.[45] Fibrils were used upon inducing production or aliquoted and stored at −80 °C. For all species, frozen and fresh material did not show any difference in ligand binding behavior.

4.18. Compound preparation

Stock solutions (34.9 mM) in DMSO of the *E* and *Z* geometric isomers of the fluorinated styryl benzazole **1–4** isomers were prepared in the dark, before dilution into assay buffer (Tris–HCl, 50 mM, pH 7.4).

4.19. Intrinsic Fluorescence Characterization

The excitation and emission wavelength scan of the *E* and *Z* isomers of compounds **1–4** were recorded in a plate reader (Tecan Infinite 200, Mannendorf, Switzerland) in the presence of monomeric or fibrillary species of insulin, α-syn, Aβ(1–42) peptide and BSA (5 μM). The maximum excitation and emission wavelength was determined according to the maximum fluorescence intensity level.

4.20. Intrinsic fluorescence intensity binding assays

Intrinsic fluorescence intensity changes associated with ligand binding to insulin, α-syn, Aβ(1–42) peptide fibrils and BSA were recorded in a plate reader (Tecan Infinite 200, Mannendorf, Switzerland). The assays were performed using different fixed concentrations of fibrils (3.5–11.35 μM) and varying concentrations of ligands **1–4** *E*/*Z* isomers (0–20 μM) at the maximum determined excitation and emission wavelengths (table 1, and supplementary data Table 1). To correct for the minimal fluorescence background, the intrinsic fluorescence of the dye blanks were determined at each explored concentration and subtracted to all data presented.[32,46,47] Resulting corrected intensities were plotted and the Kd values determined by fitting a single site saturated curve to the data using SigmaPlot™ 11.0 software. For purposes of comparison the binding assays were also performed for ThT.

Acknowledgements

The authors thank Dr Joaquim Marçalo for Mass Spectroscopy measurements, and Prof Giuseppe Ermondi and Dr Mauro Ravera for calculations of the octanol/water coefficient partition (Log*P*o/w). This work was funded by Fundação para a Ciência e Tecnologia (FCT), Portugal (PTDC/QUI/102049/2008). TFO is also supported by a Marie Curie International Reintegration Grant from the European Commission (Neurofold) and by an EMBO Installation Grant. GRM thanks the FCT for the 'Ciência 2008' program and DAAD program (0811983). HVM is supported by the FCT, Portugal (SFRH/BPD/64702/2009)

Supplementary data

Supplementary data associated with this article can be found, in the online version, at doi:10.1016/j.bmc.2011.09.065.

References and notes

1. Bacskai, B. J.; Hickey, G. A.; Skoch, J.; Kajdasz, S. T.; Wang, Y.; Huang, G. F.; Mathis, C. A.; Klunk, W. E.; Hyman, B. T. *Proc Natl Acad Sci U.S.A.* **2003**, *100*, 12462.

2. Ye, L.; Velasco, A.; Fraser, G.; Beach, T. G.; Sue, L.; Osredkar, T.; Libri, V.; Spillantini, M. G.; Goedert, M.; Lockhart, A. *J. Neurochem.* **2008**, *105*, 1428.
3. Rowe, C. C.; Ng, S.; Ackermann, U.; Gong, S. J.; Pike, K.; Savage, G.; Cowie, T. F.; Dickinson, K. L.; Maruff, P.; Darby, D.; Smith, C.; Woodward, M.; Merory, J.; Tochon-Danguy, H.; O'Keefe, G.; Klunk, W. E.; Mathis, C. A.; Price, J. C.; Masters, C. L.; Villemagne, V. L. *Neurology* **2007**, *68*, 1718.
4. Kung, H. F.; Choi, S. R.; Qu, W.; Zhang, W.; Skovronsky, D. *J. Med. Chem.* **2010**, *53*, 933.
5. van den Berg, D.; Zoellner, K. R.; Ogunrombi, M. O.; Malan, S. F.; Terre'Blanche, G.; Castagnoli, N.; Bergh, J. J.; Petzer, J. P. *Bioorg. Med. Chem.* **2007**, *15*, 3692.
6. Prousek, J. *Collect Czech. Chem. Commun.* **1991**, *56*, 1358.
7. Zhang, G. H.; Wu, F. I.; Jiang, X. Q.; Sun, P. P.; Cheng, C. H. *Synth. Met.* **2010**, *160*, 1906.
8. Hranjec, M.; Kralj, M.; Piantanida, N.; Sedic, M.; Suman, L.; Pavelic, K.; Karminski-Zamola, G. *J. Med. Chem.* **2007**, *50*, 5696.
9. Popov, I. I. *Chem. Heterocycl. Compd.* **1997**, *33*, 949.
10. Petzer, J. P.; Steyn, S.; Castagnoli, K. P.; Chen, J. F.; Schwarzschild, M. A.; Van der Schyf, C. J.; Castagnoli, N. *Bioorg. Med. Chem.* **2003**, *11*, 1299.
11. Wang, L. Y.; Zhang, X. G.; Li, F. M.; Zhang, Z. X. *Synth. Commun.* **2004**, *34*, 2245.
12. Kabatc, J. J. B.; Orlinski, P.; Paczkowski, J. *Spectrochim. Acta Part A* **2005**, *62*, 115.
13. Caleta, I.; Mrvos-Sermek, M. G. D.; Cetina, M.; Tralic-Kulenovic, V.; Pavelic, K.; Karminski-Zamola, G. *Il Farmaco* **2004**, *59*, 297.
14. Pavlovic, G. S. Z.; Popovic, Z.; Tralic-Kulenovic, V. *Polyhedron* **2007**, *26*, 5162.
15. Vasilev, A.; Deligeorgiev, T.; Gadjev, N.; Kaloyanova, S.; Vaquero, J. J.; Alvarez-Builla, J.; Baeza, A. G. *Dyes Pigments* **2008**, *77*, 550.
16. Shimadzu, H.; Suemoto, T.; Suzuki, M.; Shiomitsu, T.; Okamura, N.; Kudo, Y.; Sawada, T. *J. Labelled Comp. Radiopharm.* **2004**, *47*, 181.
17. Amatsubo, T.; Morikawa, S.; Inubushi, T.; Urushitani, M.; Taguchi, H.; Shirai, N.; Hirao, K.; Kato, M.; Morino, K.; Kimura, H.; Nakano, I.; Yoshida, C.; Okada, T.; Sano, M.; Tooyama, I. *Neurosci. Res.* **2009**, *63*, 76.
18. Fayed, T. A. *J. Photochem. Photobiol. A* **1999**, *121*, 17.
19. Cho, C. S.; Kim, D. T.; Zhang, J. Q.; Ho, S. L.; Kim, T. J.; Shim, S. C. *J. Heterocycl. Chem.* **2002**, *39*, 421.
20. Yang, X.-L.; Xu, C.-M.; Lin, S.-M.; Chen, J.-X.; Ding, J.-C.; Wu, H.-Y.; Su, W.-K. *J. Braz. Chem. Soc.* **2010**, *21*, 37.
21. Dondoni, A.; Fantin, G.; Fogagnolo, M.; Medici, A.; Pedrini, P. *Tetrahedron* **1988**, *44*, 2021.
22. Lau, C. K.; Dufresne, C.; Gareau, Y.; Zamboni, R.; Labelle, M.; Young, R. N.; Metters, K. M.; Rochette, C.; Sawyer, N.; Slipetz, D. M.; Charette, L.; Jones, T.; Mcauliffe, M.; Mcfarlane, C.; Fordhutchinson, A. W. *Bioorg. Med. Chem. Lett.* **1995**, *5*, 1615.
23. Sharghi, H.; Asemani, O. *Synth. Commun.* **2009**, *39*, 860.
24. Burkholder, C. R.; Dolbier, W. R.; Medebielle, M. *J. Fluorine Chem.* **2000**, *102*, 369.
25. Qu, W. C.; Kung, M. P.; Hou, C.; Benedum, T. E.; Kung, H. F. *J. Med. Chem.* **2007**, *50*, 2157.
26. Watanabe, M.; Morais, G. R.; Mataka, S.; Ideta, K.; Thiemann, T. Z. *Naturfor. B* **2005**, *60*, 909.
27. Suemoto, T.; Okamura, N.; Shiomitsu, T.; Suzuki, M.; Shimadzu, H.; Akatsu, H.; Yamamoto, T.; Kudo, Y.; Sawada, T. *Neurosci. Res.* **2004**, *48*, 65.
28. Lee, C. W.; Zhuang, Z. P.; Kung, M. P.; Plossl, K.; Skovronsky, D.; Gur, T.; Hou, C.; Trojanowski, J. Q.; Lee, W. M. Y.; Kung, H. F. *J. Med. Chem.* **2001**, *44*, 2270.
29. Vassar, P. S.; Culling, C. F. *Arch. Pathol.* **1959**, *68*, 487.
30. Biancalana, M.; Koide, S. *Biochim. Biophys. Acta* **2010**, *1804*, 1405.
31. Groenning, M. *J. Chem. Biol.* **2010**, *3*, 1.
32. LeVine, H., 3rd *Protein Sci.* **1993**, *2*, 404.
33. Lockhart, A.; Ye, L. A.; Morgenstern, J. L.; Lamb, J. R. *Biochem. Biophys. Res. Commun.* **2006**, *347*, 669.
34. Ye, L.; Morgenstern, J. L.; Gee, A. D.; Hong, G.; Brown, J.; Lockhart, A. *J. Biol. Chem.* **2005**, *280*, 23599.
35. Bertoncini, C. W.; Celej, M. S. *Curr. Protein Pept. Sci.* **2011**, *12*, 205.
36. Kung, H. F.; Lee, C. W.; Zhuang, Z. P.; Kung, M. P.; Hou, C.; Plossl, K. *J. Am. Chem. Soc.* **2001**, *123*, 12740.
37. Halgren, T. *J. Comp. Chem.* **1996**, *17*, 490.
38. SADABS, W. *Area-Detector Absorption Correction. Brukee AXS Inc., Madison, WI* 2004.
39. SAINT, M. *Area-Detector Integration Software. (version 7.23) Brukee AXS Inc., Madison, WI* 2004.
40. Altomare, A.; Burla, M. C.; Camalli, M.; Cascarano, G. L.; Giacovazzo, C.; Guagliardi, A.; Moliterni, A. G. G.; Polidori, G.; Spagna, R. *J. Appl. Crystallogr.* **1999**, *32*, 115.
41. Sheldrick, G. M. SHELXL-*97: Program for the refinement of Crystal Structure*; University of Gottingen: Germany, 1997.
42. Farrugia, L. J. *J. Appl. Crystallogr.* **1999**, *32*, 837.
43. Farrugia, L. J. *J. Appl. Crystallogr.* **1997**, *30*, 565.
44. Huang, C.; Ren, G.; Zhou, H.; Wang, C. C. *Protein Expr. Purif.* **2005**, *42*, 173.
45. Nilsson, M. R. *Methods* **2004**, *34*, 151.
46. Ahmad, A.; Uversky, V. N.; Hong, D.; Fink, A. L. *J. Biol. Chem.* **2005**, *280*, 42669.
47. Kumar, S.; Singh, A. K.; Krishnamoorthy, G.; Swaminathan, R. *J. Fluoresc.* **2008**, *18*, 1199.